Research Article   Open Access

Age-related histomorphometrical changes of rat's humerus

Hussien Elkhateeb, Elsayed S. I. Mohammed, Dalia Mohamedien, Yasser A. Ahmed and Soha A. Soliman*

Department of Histology, Faculty of Veterinary Medicine, South Valley University, Qena 83523, Egypt

Abstract

Previous research divided long bone growth into intramembranous and endochondral ossification. The latter contributes to longitudinal bone growth through the addition of new bone tissue at the physeal growth plate. Bones, also, increase in thickness through appositional bone growth of the cortical bone. The aim of the present study was to investigate the age-related histomorphometrical changes that occur during the growth of the humerus in rats as a model of the long bone. Samples were collected for light microscopy from the right humerus at 3, 4, 6, 8, 10, 13, and 20 weeks (wks) of age. Histological investigation revealed that the distal physeal growth plate could be detected at 3 wks of age, while at 4 wks of age it was replaced by bone trabeculae. Morphometrically, differences were observed in the thickness of the proximal physeal growth plate, specifically its proliferative zone. The thickness of the proliferative zone initially decreased, then showed a significant increase around the age of puberty (6–8 wks), then decreased significantly from 8–20 wks of age. The mid-shaft cortical bone thickness showed a significant increase during the study. In conclusion, ageing affected both longitudinal and appositional growth, which both participated in the growth and development of the rat's humerus.

Keywords: Cortical bone, Growth plate, Hypertrophic zone, Long bone, Proliferating zone.

Citation: Elkhateeb et al., Age-related histomorphometrical changes of rat's humerus. SVU-IJVS 2023, 6(2): 44-54.

Competing interest: The authors have declared that no competing interest exists.

Introduction

The skeleton has various functions. The bones of the skeleton provide mechanical and structural support for all body organs and systems and play a role in the protection of vital internal organs such as the lungs, heart, and brain. In addition, bones provide levers for the muscles that permit movement and locomotion. Furthermore, bones are an important site for hematopoiesis within the bone marrow and maintain mineral homeostasis and acid-base balance in the body (Taichman, 2005).

Morphologically, there are four general types of bones: long, short, flat, and irregular bones (Wolde-Semait and Komlos, 2020). The long bones are composed of an elongated shaft, or diaphysis, that encloses a cavity containing bone marrow, a cone-shaped metaphysis that is demarcated by the growth plates, and a convex epiphysis above the growth plates. The diaphysis is composed primarily of compact bone, whereas the metaphysis and epiphysis are composed of spongy trabecular bone lined by a relatively thin layer of dense compact bone. Considering the previous features, the humerus is regarded as a model of a long bone (Clarke, 2008).

According to the relative proportion and organization of collagen fibers and mineral contents, there are three types of bone: woven or immature bone, cortical or compact bone, and spongy or trabecular bone, which is intermediate in properties (Hench and Larry, 2005). Initially, collagen fibers are deposited in a random manner, referred to as "woven bone," and then collagen fibers begin to be deposited in a parallel orientation, referred to as "cortical bone," which is synthesized on the woven bone scaffold and characterized by its higher strength than woven bone (Shapiro *et al.*, 2019).

Long bones grow in two ways, increasing in thickness and length, known as appositional and longitudinal bone growth, respectively. Increasing the thickness of the bone occurs by deposition of bone matrix peripherally, while elongation of the bone originates in the metaphysis, particularly the growth plate, through a process called intra-cartilaginous ossification, in which cartilage is replaced by ossified matrix (Estefa and Jordi, 2020). Long bone growth originates from a structure called the epiphyseal growth plate that is formed after the appearance of secondary ossification centers. The growth plate is a cartilaginous disc that demarcates between the epiphysis and metaphysis. At the epiphyseal growth plate, intracartilaginous ossification takes place, in which zones of cartilage matrix are successively occupied by new ossified matrix. Consequently, the diaphyseal shaft elongates by the continuous depositing of ossified tissue into the transitional metaphysis. (Scheuer and Black, 2000). Postnatal development of humerus varies among different species, as the appearance and establishment of the secondary ossification center/s, the time of closure and union of the proximal and distal growth plates and the rate of longitudinal growth of the humerus (Zoetis *et al.*, 2003).

The aim of the present study was to investigate the histomorphometrical changes that occur at different ages during the development of a rat's humerus as a model of a long bone.

Materials and methods

Ethical Approval and Animal Research

Reporting of In Vivo Experiments *(ARRIVE)* Guidelines

The current study was conducted in accordance with the Egyptian Animals' Laws and the Ethical Committee of South Valley University (approval No. No.49/13.09.2022).

Experimental animals

A total number of 52 healthy male rats (Wistar Rat) were used ranging from 3 wks to 20 wks of age. Animals were purchased from a local animal house. The rats underwent the acclimatization process for 14 days before sacrifice at temperature of 25-30°C, acquired distilled drinking water and 16% pelleted ration. Three rats were sacrificed by slaughtering using sharp scalpel at each time point (3, 4, 6, 8, 10, 13, 20 wks).

Experimental design and tissue collection

The humeri of the rats were collected from the sacrificed rats by its sharp dissection from its surrounding flesh and fixed in 4% neutral buffered formalin for at least 48 hours before being decalcified by immersion in formic acid-formalin solution (5 ml formic acid added to 10 ml 40% formalin in 85 ml distilled water) for 3, 4, 12, 13, 40 and 45 days in case of ages 3, 4, 6, 8, 10-13 and 20 wks, respectively.

Time point	Decalcification time
3 wks	3 days
4 wks	4 days
6 wks	12 days
8 wks	13 days
10 wks	40 days
13 wks	40 days
20 wks	45 days

Samples are then dehydrated in ascending grades of alcohol: 70%, 80%, 90%, 100% I, then 100% II, cleared in xylene, and embedded in paraffin wax. Serial sections (3–4 m in thickness) were cut by an automated microtome (Leica RM2235, Leica Biosystems, Germany). Harris's hematoxylin and eosin (H&E) and Crossman's trichrome stains (**Bancroft and Layton, 2013**) were used for general histological description and detection of collagen fiber-rich matrix, respectively.

Morphometrical and Statistical analysis

Height of the physeal growth plate, thickness of the proliferating zone as well as thickness of the cortical bone were measured by using a Java-based image processing program ImageJ software (ImageJ 1.53e, National Institutes of Health, USA). All data were analysed by using one-way ANOVA. Values considered significant or highly significant when P value is ≤ 0.05 or ≤ 0.01, respectively.

Results

The histological investigation revealed that the distal physeal growth plate of the rat's humerus could be detected at 3 wks of age (Figs. 1A–D), and it was represented by all endochondral ossification zones (Figs. 1C and D). The proximal physeal growth plate could also be identified, presenting all zones. No cartilage canals could be noted at this age. At 4 wks of age, the distal physeal growth plate was replaced by bone trabeculae (Figs. 1E and F).

The proximal physeal growth plate showed apparent variation in its thickness between various ages (Fig. 2). At 4 wks, its initial thickness was larger, then this area was diminished at 6 wks. A significant increase occurred around the age of puberty (8 wks), then it decreased significantly at 20 wks of age (Fig. 7).
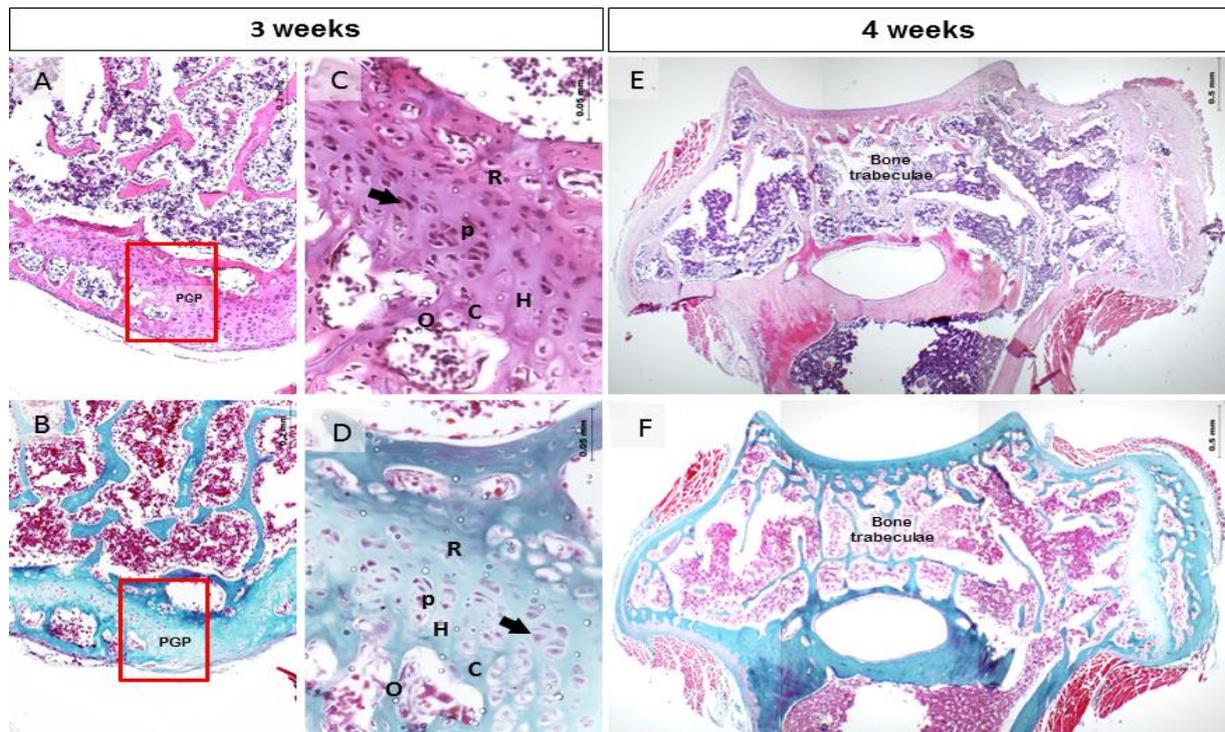
Fig. 1. Photomicrographs of distal physeal growth plate (PGP) of rats at ages 3 and 4 wks. (A), (C) and (E) stained with H&E stain, while (B), (D) and (F) stained with Crossman's trichrome stain. Arrows= proliferating chondrocytes, R= resting zone, P= proliferating zone, H= hypertrophic zone, C= calcification zone, O= ossification zone. Scale bars= 0.2 mm in (A) and (B); 0.05 mm in (C) and (D); 0.5 mm in (E) and (f).
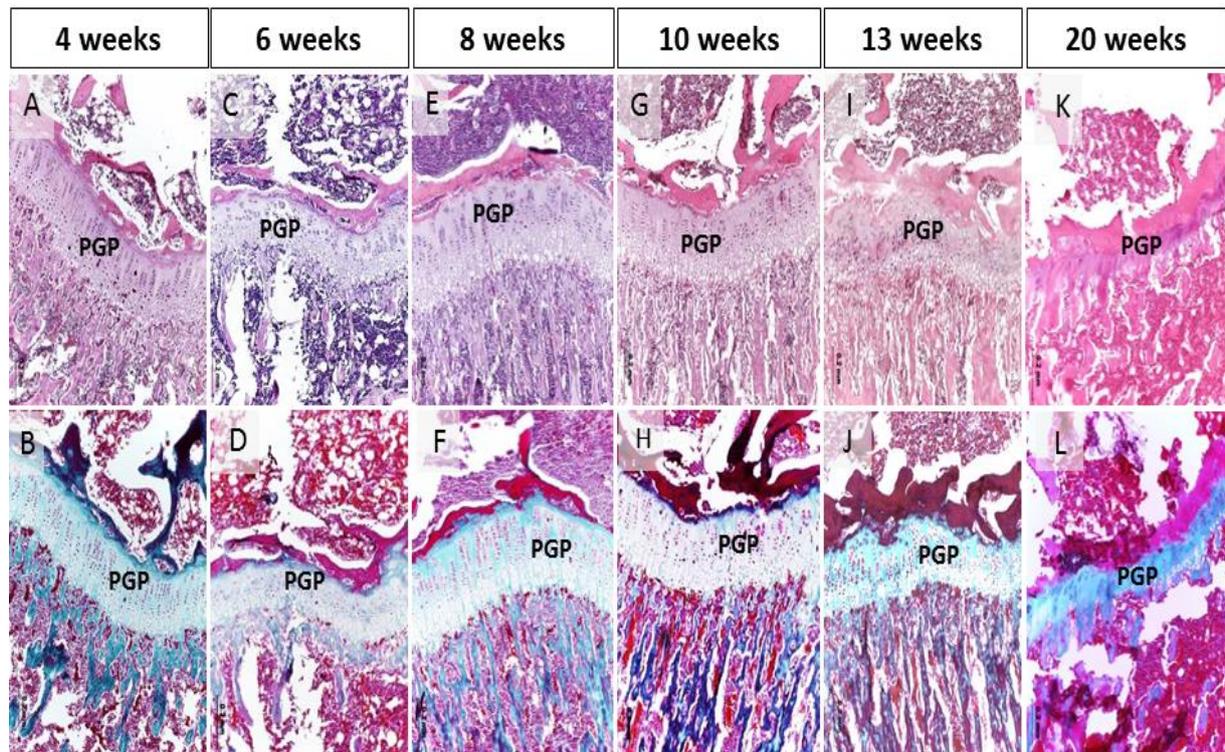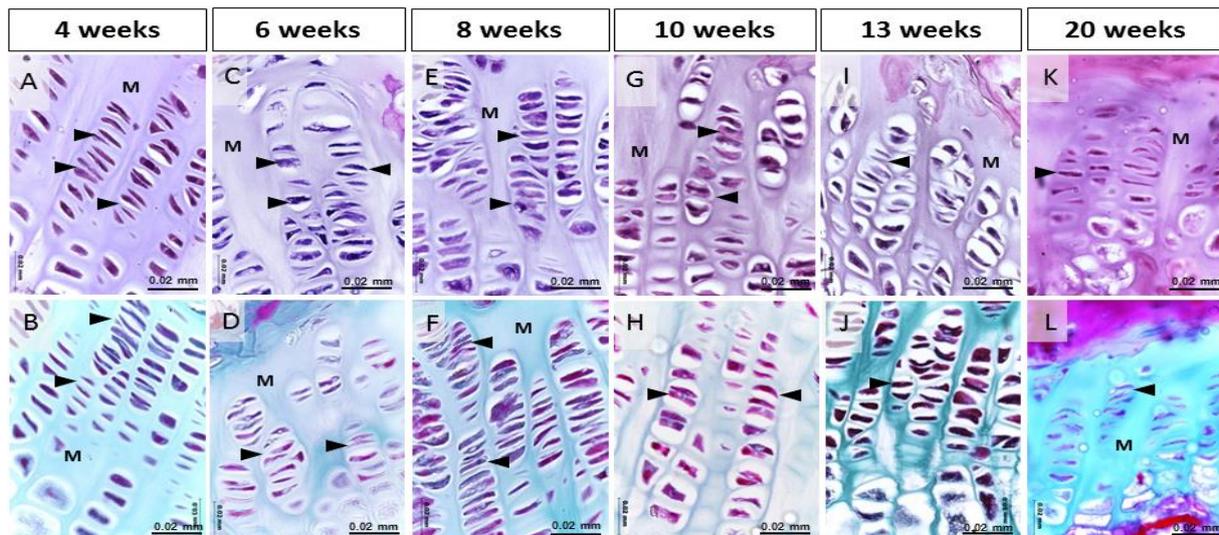

Fig. 2. Photomicrographs of proximal physeal growth plate (PGP) of rats at each time point; 4, 6, 8, 10, 13 and 20 wks. (A), (C), (E), (G), (I) and (K) stained with H&E stain, (B), (D), (F), (H), (J) and (L) stained with Crossman's trichrome stain. Scale bars= 0.2 mm in (A-L).

At higher magnification, chondrocytes were distributed in different stages in distinct and remarkable zones throughout the cartilaginous growth plate, showing the distinct zones of endochondral ossification, including resting, proliferating, hypertrophic, calcification, and ossification zones. The growth cartilage was typically organized into vertical cell columns, each of which summarized the various stages of a chondrocyte's life cycle. Chondrocytes began matrix mineralization in the longitudinal septa between cell columns during the last stages of hypertrophy (Fig. 3). The proliferating zone presented numerous chondrocytes arranged in longitudinal columns parallel to the long axis of the bone (Fig. 4).
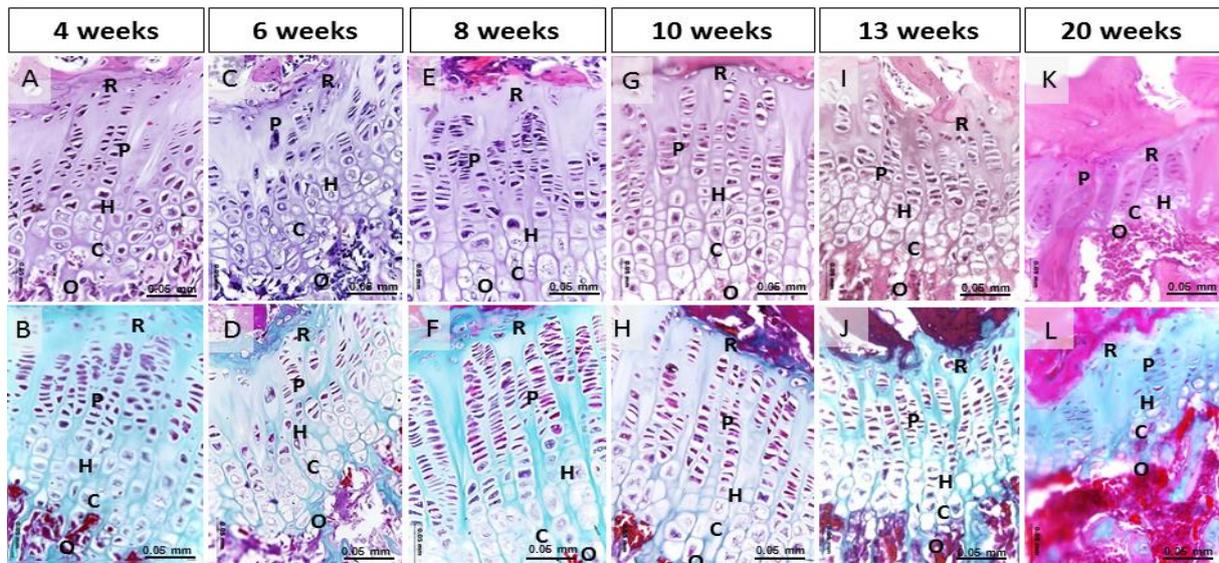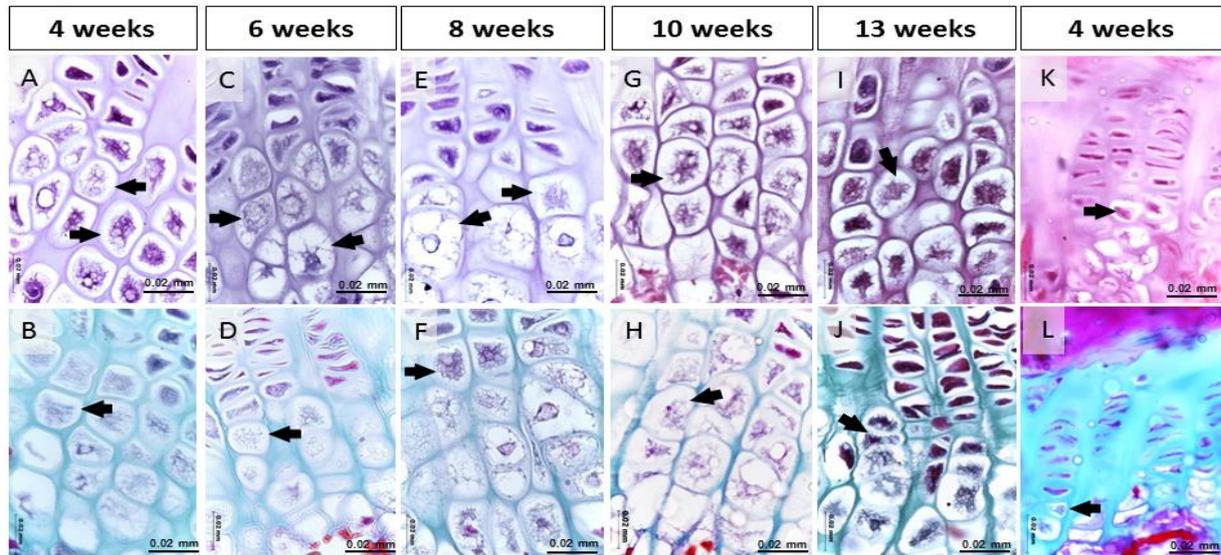

Fig. 3. Photomicrographs of proximal physeal growth plate (PGP) zones of rats at each time point; 4, 6, 8, 10, 13 and 20 wks. (A), (C), (E), (G), (I) and (K) stained with H&E stain, (B), (D), (F), (H), (J) and (L) stained with Crossman's trichrome stain. Scale bars= 0.05 mm in (A-L). R= resting zone, P= proliferating zone, H= hypertrophic zone, C= calcification zone, O= ossification zone.


Fig. 4. Photomicrographs of proliferating zone of PGP of rats at each time point; 4, 6, 8, 10, 13 and 20 wks. (A), (C), (E), (G), (I) and (K) stained with H&E stain, (B), (D), (F), (H), (J) and (L) stained with Crossman's trichrome stain. Arrowheads= proliferating chondrocytes, M= cartilage matrix. Scale bars= 0.02 mm in (A-L).

The initial thickness of the proliferating zone was larger at 3 wks of age, then it decreased at 6 wks of age. Interestingly, the thickness of the proliferating zone showed a significant increase, reaching its maximum at the age of 8 wks, then decreasing significantly from 8 to 20 wks of age to reach its minimal thickness at 20 wks of age (Fig. 8). Moving to the hypertrophic zone, in which chondrocytes have gradually undergone hypertrophy, lacunae have increased in size, and their surrounding extracellular matrix has undergone narrowing and degradation (Fig. 5).

Fig. 5. Photomicrographs of hypertrophic zone of PGP of rats at each time point; 4, 6, 8, 10, 13 and 20 wks. (A), (C), (E), (G), (I) and (K) stained with H&E stain, (B), (D), (F), (H), (J) and (L) stained with Crossman's trichrome stain. Arrows= hypertrophic chondrocytes. Scale bars= 0.02 mm in (A-L).
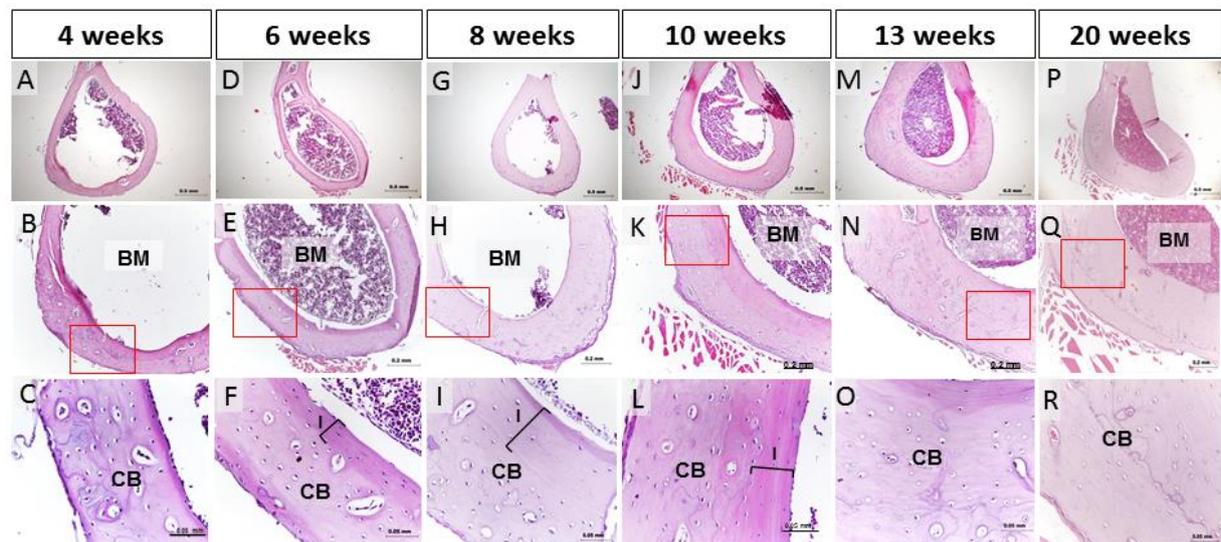
Fig. 6. Photomicrographs of mid-shaft cross section of rats at each time point; 4, 6, 8, 10, 13 and 20 wks. stained with H&E stain. BM= bone marrow, CB= cortical bone, I= inner circumferential bone lamellae. Scale bars= 0.2 mm in (A), (D), (G), (J), (M) and (P); 0.05 mm in (B), (E), (H), (K), (N) and (Q); 0.02 mm in(C), (F), (I), (L), (O) and (R).

On the other hand, the mid-shaft cortical bone thickness showed a significant age-related increase during the study period, starting from minimum thickness at the age of 3 wks to reach its maximum thickness at 20 wks of age (Figs. 6 and 9). Additionally, the cortical bone of a rat's humerus in the mid-shaft region was not built using the same Haversian system as the cortical bone of a human or large mammal. Furthermore, the inner circumferential bone lamellae showed cellular and non-vascular bone lamellae that were arranged parallel to each other (Fig. 6).
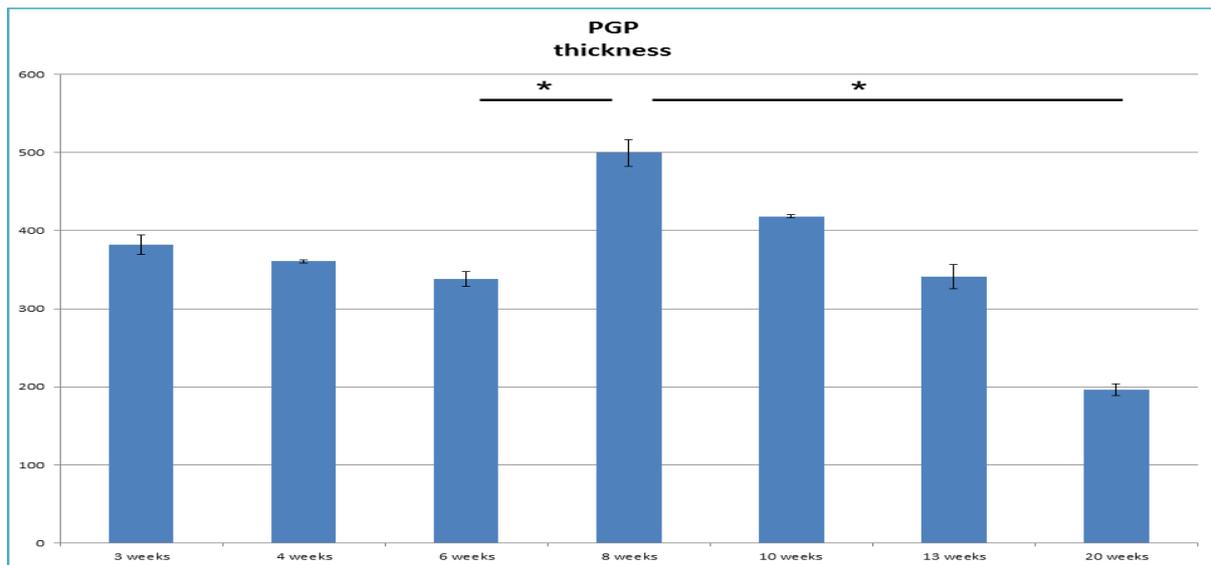

Fig. 7. The thickness of proximal physeal growth plate (PGP) of rats at each time point; 3, 4, 6, 8, 10, 13 and 20 wks. ↑ indicates increasing, ↓ indicates decreasing, (*) indicates significance

Fig. 8. The thickness of proliferating zone (PZ) of proximal physeal growth plate (PGP) of rats at each time point; 3, 4, 6, 8, 10, 13 and 20 wks. ↑ indicates increasing, ↓ indicates decreasing, (*) indicates significance.
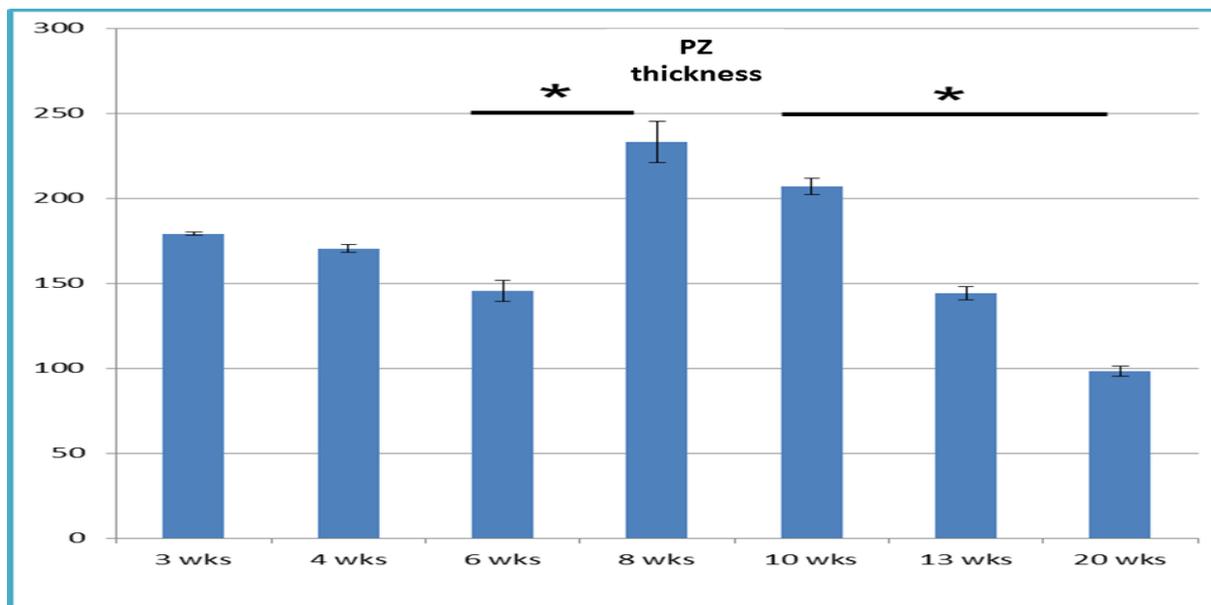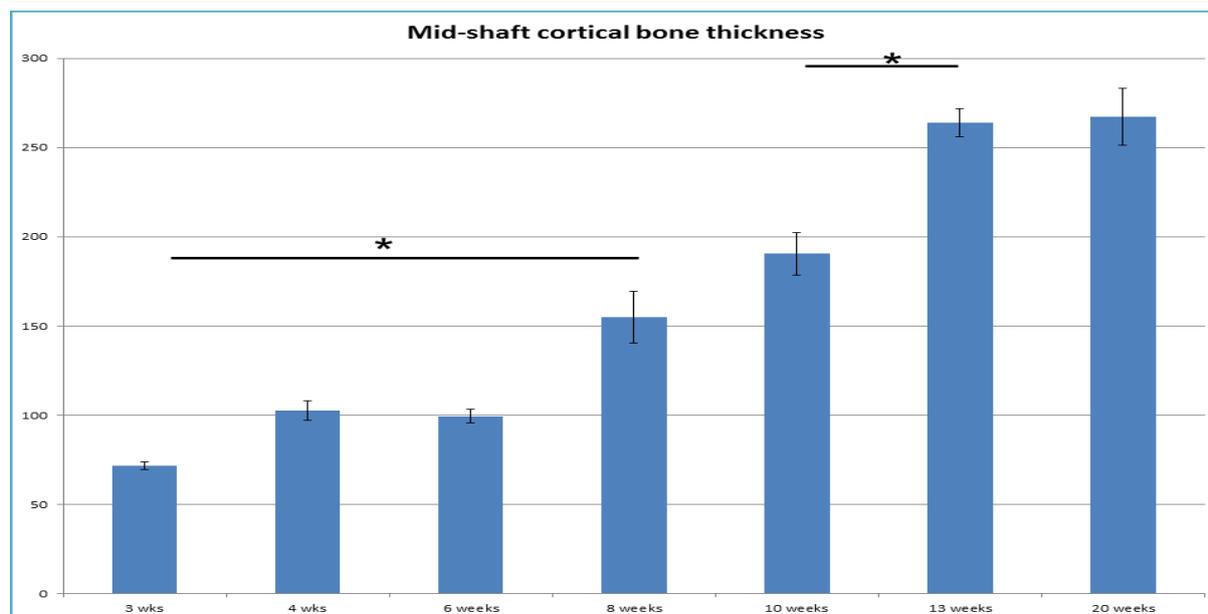
Fig. 9. The thickness of cortical bone at mid-shaft of rats at each time point; 3, 4, 6, 8, 10, 13 and 20 wks. ↑ indicates increasing, ↓ indicates decreasing, (*) indicates significance.

Discussion

We reported age-related histomorphometrical changes in the rat humerus in the current study. The major findings of this study were: (1) The cartilaginous growth plate between the distal epiphysis and metaphysis was replaced by bone trabeculae at 4 wks of age; (2) No cartilage canals could be noted at 3 wks of age; (3) The proximal physeal growth plate showed apparent variation in its thickness among various ages, and the thickness of the growth plate significantly decreased with age; (4) The proliferating zone was the main zone responsible for longitudinal bone growth; (5) No typical Haversian system could be detected in the cortical bone of the rat's humerus at mid-shaft region;

At 3 wks of age, the distal extremity showed a cartilaginous growth plate between the distal epiphysis and metaphysis, which was replaced by bone trabeculae at 4 wks of age. These findings were comparable to those obtained by Fukuda and Matsuoka, (1980); Libbin and Weinstein, (1986) and Zoetis *et al.*, (2003)

who reported that by the fourth week of age, fusion has been noticed in the distal epiphysis of the rat humerus. The first long bone epiphysis to connect with its corresponding diaphyseal shaft is the distal epiphysis of the rat humerus.

At 3 wks of age, no cartilage canals could be noted, which may be due to the establishment of the secondary ossification center. Morini *et al.,* (2004) reported that the ossification center expansion and full development of the secondary growth plate take place by 21 days of age.

The proximal physeal growth plate showed an apparent variation in its thickness among various ages, and the thickness of the growth plate was significantly decreased with age. These findings are in agreement with what had been observed by Haines, (1975), and Scheuer and Black, (2000), who reported that the epiphyseal plate starts to narrow when the rate of bone production starts to exceed the rate of cartilage proliferation, and this lead to epiphyseal fusion.

The initial thickness of the growth plate at 4 wks of age is greater than its

thickness at 6 wks of age, which may be due to the fact that the secondary ossification center is completely developed around 4-6 wks of age. This finding confirms the observations of Morini *et al.,* (2004) regarding the expansion of the secondary ossification center in the rat humeral head, which decreases or stops by the age of 5 wks. In addition, it reinforces the findings of Roach *et al.,* (2003) who observed that at an age before five weeks, the secondary ossification centre nearly did not fill the chondroepiphysis, therefore the height of the growth plate could not be regarded as being equal to the distance between the primary spongiosa of the metaphysis and the secondary ossification center. Exceptionally, in the current study, we found that the thickness of the growth plate increased significantly at the age of 8 wks. This may be due to the fact that the onset of puberty in male rats occurs at 7-8 wks of age, during which the hormones that aid in the acceleration of bone growth increase in their levels more than their levels at the prepubertal stage, which agrees with what was reported by Primus and Kellogg, (1989) and Delemarre-van de Waal *et al.,* (2002).

Interestingly, in the current investigation, we found that the proliferating zone was the main zone responsible for longitudinal bone growth, and it varied in its thickness parallel to that of the whole growth plate. That is similar to what was reported by Racine and Serrat, (2020) who stated that the proliferating zone contains multicellular columns of rapidly dividing chondrocytefurts that are stacked and flattened. The proliferating zone cells are arranged in columns, and it is a zone of actively dividing cells that controls longitudinal growth along the long axis of the bone. Within the proliferative

zone, chondrocytes' proliferative capacity declines with age, contributing to the closing of the growth plate associated with skeletal maturity. On the other hand, we found that the mid-shaft cortical bone thickness showed a significant age-related increase during the study period, due to periosteal deposition of new bone tissue, which is in agreement with the previous studies of Kincaid and Van Sickle, (1983); Fawcett, (1994), Zoetis *et al.,* (2003) Montoya-Sanhueza, *et al.,* (2021) who reported that the small rat pups have thinner cortical bone in cross section of humerus than that of juveniles which also have thinner cortical wall than that of adult individuals. Regarding the construction of cortical bone of the rat's humerus, we found that it was not constructed of typical Haversian system as that of human's and/ or large mammals' cortical bone and the inner circumferential bone lamellae showed cellular and non-vascular bone lamellae which were arranged parallel to each other. These findings agree with those reported by Duranova *et al.*, (2014); Jerome *et al.*, (2018) who suggested that, instead of the osteonal structures seen in human cortex, mouse and rat cortical bone mostly consists of circumferential lamellae and rarely exhibits the Haversian remodeling found in human bone.

In conclusion, in this study, we provided comprehensive information on the histological features of the humerus of rats at different ages. The histological structure of the rat's humerus revealed typical endochondral ossification zones, with these zones varying in thickness among themselves and at different ages. The closure time of the distal growth plate of the humerus, the thickness of the proximal growth plate, and the thickness and microstructure of the cortical bone in

the mid-shaft region all varied. This study provided baseline data on the histomorphometrical features of the growth plates of the humerus in rats at different ages, which may be useful in the identification of an unknown age or the identification of any pathological changes at these ages. Furthermore, these data form a valuable basis for comparative histology, pathology, and veterinary forensic sciences.

Acknowledgments

Conflict of interest

The authors declare that they have no conflict of interest.

Orcid No.

Hussien Elkhateeb's ORCID No.: https://orcid.org/0000-0001-6288-1331.

Elsayed S. I. Mohammed's ORCID No.: https://orcid.org/0000-0002-7884-8234.

Yasser A. Ahmed's ORCID No.: https://orcid.org/0000-0001-6727-5250.

Dalia Mohamedien's ORCID No.: https://orcid.org/0000-0003-0047-8007.

Soha A. Soliman's ORCID No.: https://orcid.org/0000-0001-6507-8405.

Financial statement

References

Bancroft, J. D. and Layton, C., 2013. Bancroft's Theory Practice of histological techniques, 7th Ed. *Philadelphia: Churchill Livingstone of El Sevier, Philadelphia, USA*.

Clarke, B., 2008. Normal bone anatomy and physiology. *Clinical journal of the American Society of Nephrology, 3*(Supplement 3), pp.S131-S139.

Libbin, R.M. and Weinstein, M., 1986. Regeneration of growth plates in the long bones of the neonatal rat hindlimb. *American journal of anatomy, 177*(3), pp.369-383.

Delemarre-van de Waal, H.A., van Coeverden, S.C. and Engelbregt, M.J., 2002. Factors affecting onset of puberty. *Hormone Research in Paediatrics, 57*(Suppl. 2), pp.15-18.

Duranova, H., Martiniakova, M., Omelka, R., Grosskopf, B., Bobonova, I. and Toman, R., 2014. Changes in compact bone microstructure of rats subchronically exposed to cadmium. *Acta Veterinaria Scandinavica, 56*(1), pp.1-8.

Estefa, J., 2020. Long bone growth and evolution revealed by three-dimensional imaging (Doctoral dissertation, *Acta Universitatis Upsaliensis*).

Fukuda, S. and Matsuoka, O., 1980. Comparative studies on maturation process of secondary ossification centers of long bones in the mouse, rat, dog, and monkey. *Experimental Animals, 29*(3), pp.317-326.

Hench, L.L., 2005. The skeletal system. In *Biomaterials, artificial organs, and tissue engineering*. Woodhead Publishing.

Jerome, C., Hoch, B. and Carlson, C.S., 2018. Skeletal system. In *Comparative Anatomy and Histology* (pp. 67-88). Academic Press.

Montoya-Sanhueza, G., Bennett, N.C., Oosthuizen, M.K., Dengler-Crish, C.M. and Chinsamy, A., 2021. Long bone histomorphogenesis of the naked mole-rat: histodiversity and intraspecific variation. *Journal of Anatomy, 238*(6), pp.1259-1283.

Morini, S., Continenza, M.A., Ricciardi, G., Gaudio, E. and Pannarale, L., 2004. Development of the microcirculation of the secondary ossification center in rat humeral head. *The Anatomical Record Part A: Discoveries in Molecular, Cellular, and Evolutionary Biology: An Official Publication of the American Association of Anatomists, 278*(1), pp.419-427.

Primus, R.J., and Kellogg, C.K., 1989. Pubertal related changes influence the development of environment related social interaction in the male rat. *Developmental Psychobiology: The Journal of the International Society for Developmental Psychobiology, 22*(6), pp.633-643.

Racine, H.L. and Serrat, M.A., 2020. The actions of IGF-1 in the growth plate and its role in postnatal bone elongation. *Current osteoporosis reports, 18*(3), pp.210-227.

Roach, H.I., Mehta, G., Oreffo, R.O., Clarke, N.M. and Cooper, C., 2003. Temporal analysis of rat growth plates: cessation of growth with age despite presence of a physis. *Journal of Histochemistry & Cytochemistry, 51*(3), pp.373-383.

Scheuer, L. and Black, S., 2000. Development and ageing of the juvenile skeleton. *Human osteology in archaeology and forensic science*, pp.9-22.

Shapiro, F., and Wu, J.Y., 2019. Woven bone overview: Structural classification based on its integral role in developmental, repair and pathological bone formation throughout vertebrate groups. *Eur. Cell. Mater,* 38, pp.137-167.

Taichman, R.S., 2005. Blood and bone: two tissues whose fates are intertwined to create the hematopoietic stem-cell niche. *Blood, 105(7)*, pp.2631-2639.

Wolde-Semait, H.T. and Komlos, D., 2020. Normal Bone Physiology. In *Vertebral Compression Fractures in Osteoporotic and Pathologic Bone* (pp. 1-8). Springer, Cham.

Zoetis, T., Tassinari, M.S., Bagi, C., Walthall, K. and Hurtt, M.E., 2003. Species comparison of postnatal bone growth and development. *Birth Defects Research Part B: Developmental and Reproductive Toxicology, 68*(2), pp.86-110.